HHS Public Access

Author manuscript

Diabetologia. Author manuscript; available in PMC 2019 March 30.

Published in final edited form as:

Diabetologia. 2019 March ; 62(3): 504–516. doi:10.1007/s00125-018-4773-1.

Anti-fumarase antibody promotes the dropout of photoreceptor inner and outer segments in diabetic macular oedema

Shin Yoshitake[1], **Tomoaki Murakami**[1], **Kiyoshi Suzuma**[1], **Tatsuya Yoshitake**[1], **Akihito Uji**[1], **Satoshi Morooka**[1], **Yoko Dodo**[1], **Masahiro Fujimoto**[1], **Yang Shan**[2], **Patrice E. Fort**[2,3], **Shinji Ito**[4], **Akitaka Tsujikawa**[1], and **Nagahisa Yoshimura**[1]

[1]Department of Ophthalmology and Visual Sciences, Kyoto University Graduate School of Medicine, 54 Shogoin-Kawaracho, Sakyo, Kyoto 606-8507, Japan

[2]Department of Ophthalmology and Visual Sciences, University of Michigan, Kellogg Eye Center, Ann Arbor, MI, USA

[3]Department of Molecular and Integrative Physiology, University of Michigan, Kellogg Eye Center, Ann Arbor, MI, USA

[4]Medical Research Support Center, Graduate School of Medicine, Kyoto University, Kyoto, Japan

Abstract

Aims/hypothesis—In diabetic macular oedema (DMO), blood components passing through the disrupted blood-retinal barrier cause neuroinflammation, but the mechanism by which autoantibodies induce neuroglial dysfunction is unknown. The aim of this study was to identify a novel autoantibody and to evaluate its pathological effects on clinically relevant photoreceptor injuries.

Methods—Biochemical purification and subsequent peptide fingerprinting were applied to identify autoantigens. The titres of autoantibodies in DMO sera were quantified and their associations with clinical variables were evaluated. Two animal models (i.e. passive transfer of autoantibodies and active immunisation) were characterised with respect to autoimmune mechanisms underlying photoreceptor injuries.

Results—After screening serum IgG from individuals with DMO, fumarase, a Krebs cycle enzyme expressed in inner segments, was identified as an autoantigen. Serum levels of anti-fumarase IgG in participants with DMO were higher than those in diabetic participants without

Tomoaki Murakami mutomo@kuhp.kyoto-u.ac.jp.

Contribution statement

SY conceived and designed the study, acquired data, drafted the manuscript and approved its final version. TM, KS, TY, AU, SM, YD, MF, AT and NY contributed to the conception and design of the study and acquisition, analysis and interpretation of data, revised the article's intellectual content and approved the final version. YS, PEF and SI contributed to the acquisition and analysis of data, revised the article's intellectual content and approved the final version. TM is the guarantor of this work.

Data availability

All data generated or analysed during this study are included in this published article and its supplementary information files.

Duality of interest

The authors declare that there is no duality of interest associated with this manuscript.

Electronic supplementary material The online version of this article (https://doi.org/10.1007/s00125–018-4773–1) contains peer-reviewed but unedited supplementary material, which is available to authorised users

DMO ($p < 0.001$) and were related to photoreceptor damage and visual dysfunction. Passively transferred fumarase IgG from DMO sera in concert with complement impaired the function and structure of rodent photoreceptors. This was consistent with complement activation in the damaged photoreceptors of mice immunised with fumarase. Fumarase was recruited to the cell surface by complement and reacted to this autoantibody. Subsequently, combined administration of anti-fumarase antibody and complement elicited mitochondrial disruption and caspase-3 activation.

Conclusions/interpretation—This study has identified anti-fumarase antibody as a serum biomarker and demonstrates that the generation of this autoantibody might be a pathological mechanism of autoimmune photoreceptor injuries in DMO.

Keywords

Anti-fumarase antibody; Autoantibody; Complement; Diabetic macular oedema; Optical coherence tomography; Photoreceptor damage; Serum biomarker

Introduction

Diabetic retinopathy often leads to severe vision loss [1, 2]. An increasing number of studies have determined that disturbances in both vascular cells and neuroglial components reciprocally promote the pathogenesis of diabetic retinopathy [3–5]. In particular, diabetes mellitus exacerbates blood- retinal barrier (BRB) breakdown and concomitant diabetic macular oedema (DMO), which often leads to severe vision disturbances. However, it remains largely unknown how the extravasated blood components damage neuroglial cells.

Advances in optical coherence tomography (OCT) have enabled clinicians to evaluate retinal status [6]. Retinal thickening in the macula is one of the major indicators of DMO [7], and high-resolution OCT enables assessment of the status of the ellipsoid zone of the photoreceptors as a representative of photoreceptor integrity. Histologically, this region contains a high number of mitochondria that support the increased level of metabolism of photoreceptor cells [8]. In eyes with DMO the ellipsoid zone line is often disrupted, which significantly correlates with vision impairment [9, 10]. However, the molecular or cellular mechanisms behind the photoreceptor damage must be elucidated in order to establish novel therapeutic strategies for DMO [11, 12].

Subretinal spaces are limited by the barrier properties of the external limiting membrane and the retinal pigment epithelium and, in healthy retinas, are known to be isolated from immunity (‘immunoprivileged’) [13]. In chorioretinal diseases, impairment of neurovascular units leads to microvascular pathogenicity and neuroinflammation, as seen in neurological diseases [14]. In cancer-associated retinopathy (CAR), autoantibodies against proteins expressed in photoreceptor cells, such as recoverin and arrestin, contribute to progressive photoreceptor degeneration [15]. This evidence encouraged us to speculate that BRB breakdown in diabetic eyes might lead to neuroglial damage through various neurotoxic blood components, including immunological agents, which is to some extent supported by publications regarding the recruitment and activation of inflammatory cells in chorioretinal diseases [16, 17].

In the current study, we aimed to identify autoantibodies against photoreceptor cells in a subgroup of individuals with DMO and to investigate their contribution to photoreceptor damage.

Methods

Participants and biosampling

Participants with type 2 diabetes were consecutively recruited at the Department of Ophthalmology of Kyoto University Hospital and divided into the following three groups: (1) DM group, comprising participants with type 2 diabetes but not diabetic retinopathy; (2) DR group, comprising participants with diabetic retinopathy but not centre-involved DMO; and (3) DMO group, comprising participants with centre-involved DMO.

In the discovery cohort recruited from July 2014 to February 2016, we first included participants as shown in the flow chart (see electronic supplementary material [ESM] Fig. 1). Samples from these participants were used for screening by western blot or immunostaining, immunoprecipitation and subsequent MS, ELISA to measure the autoantibody titre, and animal or cell culture experiments (ESM Fig. 1). In the validation cohort for ELISA, participants were included from March 2016 to December 2017. Participants of the same sex and similar age and HbA_{1c} level to the individual groups were included in the ELISA experiments. After excluding 33 eyes with media opacity affecting visual acuity according to participants' medical records, we included 106 eyes in the DMO group of both cohorts and analysed the association of anti- fumarase IgG with other clinical variables (ESM Fig. 1). We collected serum samples in 21 participants before and after anti-vascular endothelial growth factor (anti-VEGF) treatment (with three initial consecutive monthly injections followed by an 'as-needed' phase) and evaluated the changes in autoantibody titres. The characteristics of participants in the individual studies are detailed in ESM Tables 1–10.

Sera were aliquoted within 1 h after sampling and immediately stored at −80°C. We conducted this study in accordance with the Declaration of Helsinki. The study was approved by the Kyoto University Graduate School and Faculty of Medicine Ethics Committee and registered at the UMIN Japan Clinical Trial Registry (UMIN000014015). All participants provided written informed consent before inclusion in the study. More details of the patients and biosampling are provided in ESM Methods.

Enrichment of photoreceptor cells

Eyeballs from dead pigs were obtained from an abattoir and stored on ice soon after slaughter. After the isolation of the retinas, photoreceptor cells from porcine retinas were prepared by centrifugation in a stepwise Percoll gradient (see ESM Methods).

Cell culture and gene knockout

Human embryonic kidney (HEK) 293 cells and 661W cells were cultured. The gene encoding fumarate hydratase (FH) was knocked out in HEK 293 cells using the CRISPR/Cas9 system (see ESM Methods).

Animals

After approval by the institutional review board of the Kyoto University Graduate School of Medicine, wildtype or *Ins2Akita* C57BL/6 mice and C57BL/10.RIII-H2^{r} *H2-T18*^{b}*/(71NS)SnJ* (B10.RIII) mice were housed in accordance with the Institutional Animal Care and Use Committee guidelines as well as with the Association for Research in Vision and Ophthalmology Statement for Use of Animals in Ophthalmic and Vision Research. Eyes were harvested under a lethal dose of anaesthesia. The exclusion criterion was based on the media opacity, which affects the in vivo assessment. We performed subretinal injections of 290 eyes and excluded 14 eyes with media opacities (see ESM Methods).

PCR

The mRNA expression of murine *Fh* (also known as *Fhl;* accession number: NM_010209.2) in retinas from C57BL/6 mice (wild-type or /*Ins*2Akita diabetic) was determined using PCR (see ESM Methods).

Immunoblot analysis

Porcine retinal lysates were applied to SDS-PAGE. Sera from participants were incubated as primary antibodies to detect retinal autoantigens.

We evaluated protein levels of fumarase in HEK 293 cells and levels of cytochrome C, apoptosis-inducing factor and β-actin in the cytosolic fraction of 661W cells using commercially available antibodies (ESM Table 11). The antibodies were used according to the manufacturers' instructions. See ESM Methods for more information.

Immunoprecipitation

Cell lysates of porcine photoreceptor cells were incubated with serum IgG conjugated to protein G-coated beads to immunoprecipitate antigens against autoantibodies (see ESM Methods).

MS

After in-gel digestion of immunoprecipitated proteins from porcine photoreceptor cells, tryptic digests were introduced into a mass spectrometer (see ESM Methods).

Preparation of cytosol fractions

Cytosol fractions were prepared from 661W cells using a subcellular fractionation kit (Mitochondria Isolation Kit for Cultured Cells; Thermo Scientific, Waltham, MA, USA) (see ESM Methods).

Measurements of the intracellular Ca^{2+} concentration

The intracellular Ca^{2+} concentration was measured using a Fluo 4-AM kit (Calcium kit-Fluo 4; Dojindo Laboratories, Tokyo, Japan) in 661W cells (see ESM Methods).

Measurements of mitochondrial membrane potential

After incubation with JC-1 dye (Thermo Scientific), fluorescence levels were measured in HEK 293 cells according to the manufacturer's protocol (see ESM Methods).

Caspase-3 activity

Caspase-3 activity in 661W cells was assessed by the colorimetric assay (APOPCYTO Caspase-3 Colorimetric Assay Kit; MBL, Aichi, Japan) (see ESM Methods).

Flow cytometry

After HEK 293 or 661W cells had been incubated with fluorescence-labelled anti-fumarase antibody, the fluorescence intensity was analysed using FACSCalibur (BD Biosciences, San Jose, CA, USA) (see ESM Methods).

ELISA

Wells in which the bottom was coated with recombinant human fumarase were incubated in diluted serum as the primary antibodies (see ESM Methods).

Antibody depletion and subretinal injection of serum

Agarose beads conjugated to recombinant human fumarase were incubated with DMO sera to prepare sera depleted of anti-fumarase antibodies. These specimens were injected into the subretinal spaces in C57BL/6 mice (see ESM Methods).

Purification of anti-fumarase antibodies from DMO sera and preparation of complement components

Anti-fumarase antibodies from DMO sera were captured using NHS-Activated Sepharose 4 Fast Flow (GE Healthcare, Piscataway, NJ, USA) coupled to human recombinant fumarase. The purified auto-antibodies were administered into the subretinal spaces in C57BL/6 mice (passive transfer model; see ESM Methods).

Immunisation with fumarase

B10.RIII mice were immunised using fumarase in combination with complete Freund's adjuvant and pertussis toxin (active immunisation model; see ESM Methods).

Immunostaining

Retinal sections from mice (C57BL/6 wildtype, C57BL/6 *Ins*2Akta or B10.RIII) retinas were incubated with DMO sera or antibodies against cytochrome C oxidase (COX) IV, fumarase, recoverin, CD59a and C5b-9, followed by fluorescence-labelled secondary antibodies (ESM Table 11). Human retinas from deceased donors were obtained from Eversight (https://www.eversightvision.org/researchers/ researcher/#request-tissue; see ESM Table 4 for donor details) and were stained with anti-fumarase antibody. HEK 293 or 661W cells were also incubated with primary antibodies against fumarase and C5b-9 (ESM Table 11).

Electron microscopy

Ultrathin slices of HEK 293 cells were observed by transmission electron microscopy (H-7650; Hitachi, Tokyo, Japan) (see ESM Methods).

Cell viability assay

Treated HEK 293 or 661W cells were applied to a cell viability/cytotoxicity assay kit (LIVE/DEAD assay; Life Technologies, Gaithersburg, MD, USA) according to the manufacturer's instructions (see ESM Methods).

Electroretinogram

Amplitudes of the mixed cone and rod responses were evaluated in C57BL/6 mice (see ESM Methods).

OCT

After retinal sectional images were obtained using spectral domain OCT in participants with diabetic retinopathy, we evaluated the central subfield thickness, ellipsoid zone status and disorganisation ofthe retinal inner layers. Spectral domain OCT images of C57BL/6 mice were also acquired (see ESM Methods).

Statistics

No experiments were randomised. All experiments were blind to group assignment and outcome assessment. After confirming normality with the Kolmogorov-Smirnov test, the Kruskal-Wallis test of ANOVA with Dunnett's multiple comparison, Mann-Whitney U test or Wilcoxon signed- rank test was performed to evaluate non-parametric data. Spearman's rank correlation coefficient was used to show statistical correlations. Paired *t* tests, Student's *t* tests or one-way ANOVA with Bonferroni correction were used to assess statistical differences in parametric parameters. Sampling distributions in participants' characteristics were evaluated using Fisher's exact test or the χ^2 test. We further applied univariate or multivariate logistic and linear regression analyses. These statistical analyses were performed using commercial software (PASW Statistics, version 18; SPSS, Chicago, IL, USA), and $p < 0.05$ was considered significant. Values are shown as means ± SD.

Results

Identification of fumarase as an autoantibody target

During autoantibody screening, western blot analyses showed that serum IgG from DMO participants had high levels of immunoreactivity to proteins expressed in porcine retinas and photoreceptor cells, suggesting the presence of autoantibodies specific to individuals with DMO (Fig. 1). We therefore planned the translational research to compare OCT and immunoreactivity to retinal autoantigens (Fig. 2). Among several bands, an approximately 50 kDa band was detected in sera from 19 of 27 DMO participants (70.4%). In addition, immunostaining using serum IgG revealed specific signals in photoreceptor cells, including inner segments, of C57BL/6 mice in 23 of 27 DMO participants (85.2%) (Fig. 2).

To identify the targets of the autoantibodies in DMO serum, we performed a combination of immunoprecipitation and MS, as described previously [18]. Porcine photoreceptor lysates were immunoprecipitated with serum IgG according to protein G sepharose bead-based procedures. SDS-PAGE followed by silver staining revealed that a unique, approximately 50 kDa band was precipitated with DMO serum (Fig. 3a, b). After ingel digestion, peptide mass fingerprinting identified fumarase (predicted molecular weight 55 kDa) as an autoantigen, which was confirmed by immunoblotting using mouse monoclonal anti-fumarase antibody and recombinant human fumarase (Fig. 3 c, d).

Fumarase, one of the main metabolic enzymes of the tricarboxylic acid cycle, is transported mainly into the mitochondrial matrix, although some forms are cytosolic [19]. In the retinas of both control and diabetic mice (male heterozygous *Ins2*Akita mice), fumarase mRNA was amplified by PCR (ESM Fig. 2). Immunostaining showed that fumarase was highly expressed in photoreceptor inner segments containing accumulated mitochondria in both human and rodent retinas (Fig. 3e and ESM Fig. 2b, respectively), although there were no definite differences in its expression between control and diabetic donors.

Quantitative analyses of anti-fumarase antibody

ELISA analysis revealed that the titres of total serum IgG against fumarase from DMO participants were significantly higher than those from participants in the DM and DR groups (Fig. 4a) [20]. According to the post hoc comparisons, the titres of anti-fumarase IgG were not different among participants with moderate non-proliferative diabetic retinopathy, severe non-proliferative diabetic retinopathy and proliferative diabetic retinopathy (data not shown) [21]. Furthermore, an independent cohort confirmed that the DMO group had higher titres than the DR group (p <0.001; ESM Table 6). Multivariate logistic regression analyses indicated that the titre of anti-fumarase IgG may be a serum biomarker for a subgroup of DMO among individuals with type 2 diabetes or diabetic retinopathy (ESM Tables 12 and 13).

In 106 eyes with centre-involved DMO, the serum titre of anti-fumarase IgG was modestly correlated to logarithm of the minimum angle of resolution (logMAR) visual acuity and ellipsoid zone disruption on spectral domain OCT images, rather than to disorganisation of retinal inner layers or central subfield thickness (Fig. 4b, c, ESM Table 14). Interestingly, the titre of this autoantibody was decreased after anti-VEGF treatment (Fig. 4d).

Functional analysis of anti-fumarase antibody

These results encouraged us to investigate the in vivo effects of anti- fumarase antibody on photoreceptor damage. DMO sera with anti-fumarase antibodies were randomly selected and injected into the subretinal spaces of C57BL/6 mice (Fig. 5). Both the IgG in DMO serum and C5b-9, which is a component of the membrane attack complex (MAC) of the complement system, showed diffuse immunostaining with a punctate appearance mainly in both inner and outer segments and little cellular infiltration 24 h after the injection. In contrast, these signals were completely diminished in retinas injected with serum depleted of anti-fumarase antibodies (Fig. 5d, e).

Histological analyses revealed that outer segments and parts of inner segments, but not the outer nuclear layer, disappeared in some areas of the retinas 7 days after the administration of DMO serum containing anti-fumarase IgG. In contrast, both inner and outer segments were preserved in retinas that received sera depleted of anti-fumarase antibody. This was consistent with spectral domain OCT findings that the ellipsoid zone line was not complete and outer retinal thickness was decreased in retinas administrated DMO serum, compared with retinas injected with serum depleted of fumarase antibodies (Fig. 5f-i).

The deposition of MAC and minimal cellular infiltration in photoreceptor outer segments were consistent with the higher titres of IgG1 and/or IgG3 and the absence of CD59a, a membrane-bound inhibitor of the MAC (Figs 4e-h, 5c-e). These results encouraged us to investigate the function of anti-fumarase antibody in concert with the complement cascade among several mechanisms of autoantibody-mediated autoimmunity. We first evaluated photoreceptor damage in C57BL/6 mice in which autoantibodies and complement were passively transferred. Histological and electroretinogram experiments confirmed that the photoreceptors were morphologically and functionally ablated 7 days after subretinal injection with anti- fumarase IgG + complement, as observed in eyes injected with DMO sera, whereas these changes were not observed after injection of fumarase IgG alone or control IgG + complement (Fig. 6a-c, ESM Fig. 3). In six of 14 (42.9%) B10.RIII mice (H2r) immunised with fumarase, both haematoxylin and eosin staining and immunofluorescence delineated structural damage in the photoreceptor inner and outer segments, although cells rarely migrated into the subretinal spaces (Fig. 6d). Mouse IgG was partly co-localised with C5b-9 in the inner and outer segments (Fig. 6e).

We further planned cell culture experiments to investigate the mechanisms by which this autoantibody and complement induced cellular damage. In vitro experiments revealed that the autoantibody was partially co-localised with fumarase and C5b-9 on the cell surface after incubation with anti- fumarase IgG purified from DMO sera and complement, whereas co-staining was not observed in $FH^{-/-}$ cells (Fig. 7a, b, ESM Fig. 4a-c).

The intracellular Ca^{2+} concentration was transiently increased under control IgG and complement, as in the case of sublytic MAC-induced Ca^{2+} influx in nucleated cells [22]. High levels of Ca^{2+} influx persisted after treatment with both anti-fumarase antibody and complement, compared with no alteration of the Ca^{2+} concentration by anti-fumarase antibody alone (Fig. 7c). Ca^{2+} chelators reversed the immunoreactivity of fumarase on the cell surface (ESM Fig. 4d, e). Consistent with Ca^{2+} burst-induced mitochondrial disruption [23], the mitochondrial membrane potential was decreased and proapoptotic signal transducing molecules, cytochrome C and apoptosis-inducing factor, leaked into the cytosol under anti-fumarase antibody in combination with complement (Fig. 7d, e). Caspase-3, an apoptosis executioner, was also activated in a Ca^{2+}-dependent manner (Fig. 7f).

Transmission electron microscopy revealed multiple processes during cell death, including vacuolation in the cytosol and mitochondria as well as nuclear deformation under anti-fumarase antibody and complement (Fig. 7g) [24]. Actually, the number of dead cells increased after administration of the combination, which was reversed by *FH* gene ablation. Furthermore, this cell death partly depended on caspase-3 activation (Fig. 7h, i). Pruning of

axons and dendrites is mediated by mitochondrial damage and a caspase pathway in developmental or pathological neurons [25, 26], which might allow us to speculate that these in vitro experiments support subcellular damage of photoreceptor inner and outer segments.

Discussion

Many publications have shown that, in addition to retinal thickening, foveal photoreceptor damage is related to visual dysfunction in eyes with DMO [7, 9,10], although the cellular and molecular mechanisms are unknown. A disrupted BRB in diabetic retinas allows blood components, including autoantibodies, to pour into the extravascular space and exacerbate neuroinflammation [3, 4, 27]. In the current study, anti- fumarase autoantibody, which was newly identified in sera from a subgroup of DMO participants, was clinically associated with photoreceptor damage and vision impairment. This fumarase autoantibody, in concert with complement activation, induced the dropout of photoreceptor inner and outer segments. Our results suggest a novel target of autoantibodies in DMO sera as well as a novel pathological mechanism for photoreceptor damage, which is clinically evident on spectral domain OCT images in DMO [9, 10].

After screening using immunoblotting, in which protein denaturation provides higher sensitivity for epitopes, we used immunoprecipitation with a non-denaturing buffer (high salt concentration and neutral pH) to mimic the three-dimensional antigen-antibody reaction and to concentrate autoantigens for subsequent MS [18]. The second screening excluded many autoantigen candidates, allowing the identification of several putative antigens. Of these, fumarase was both a target for autoantibodies in DMO sera and was highly expressed in the inner segment of photoreceptors, which prompted us to focus on qualitative and quantitative analyses of anti-fumarase antibody.

According to the quantitative ELISA data, 32 of 65 participants (49.2%) with DMO had a moderate titre of anti- fumarase antibody (above the mean + 2SD in the DM group), whereas western blot detected an approximately 50 kDa band in 19 of 27 (70.4%) DMO serum. The discrepancy might depend on the different biochemical methods used to detect the different epitopes. Another possibility might be the presence of additional autoantigens with almost the samemolecular weight, such as arrestin and enolase, both of which have been reported as targets for autoantibodies in sera from individuals with CAR or age-related macular degeneration [28, 29]. Furthermore, immunoblotting revealed that IgG in DMO sera had immunoreactivity to several antigens with other molecular weights in photoreceptor cells, and immuno- staining using serum IgG also showed immunoreactivity to photoreceptor cells in 23 of 27 DMO participants (85.2%). Some participants with the lower titre of anti-fumarase IgG had photoreceptor damage and poor visual function. These results suggest additional autoantigens in photoreceptor cells. Using immunofluorescence, we often observed definite fluorescent signals in the ganglion cell layer and inner nuclear layer. Taken together, systematic analyses of anti-retinal antibodies would promote our understanding of the immunological aspects of neuroinflammation in DMO.

Statistical analyses of the clinical data demonstrated that anti-fumarase IgG was increased in a subgroup of DMO participants with photoreceptor damage and vision impairment,

although whether this autoantibody is the cause or result of photoreceptor damage remains to be determined. In vitro and in vivo experiments in the current study suggest that this autoantibody might promote photoreceptor damage in DMO. In contrast, whether autoantibody production is induced by the intracellular antigens derived from photoreceptor cells remains ill defined. We speculate that the disrupted BRB could allow retinal autoantigens to enter the blood or to recruit or activate immune cells to migrate to and from the retina [30], and a future study should elucidate the molecular mechanisms by which vascular permeability contributes to the elicitation of autoimmunity. As another possible explanation, anti-fumarase IgG might represent mitochondria-related systemic complications due to diabetes, which are clinically associated with DMO [31]. Antigen-specific regulatory T cells, which lead to immune tolerance, might be modulated by diabetic states [32]. Diabetes induces mitochondrial damage that is at least partly mediated via oxidative stress, which might contribute to the exposure of intracellular autoantigens and immunological tolerance loss by the post-translational modification of autoantigens [31–34].

Complement MAC was formed in photoreceptor inner and outer segments in the passive transfer model. This encouraged us to speculate that photoreceptor damage is mediated via complement activation at least partly among several autoantibody-related mechanisms [35, 36]. Some autoanti bodies can, by themselves, inhibit the function of antigens and concomitantly promote pathological mechanisms, as in the case of myasthenia gravis. In contrast, anti-fumarase IgG did not promote cellular injury in the absence of complement. Cell death was not increased in $FH^{-/-}$ cells, and a few publications have documented oncological findings induced by genetic mutations [37, 38]. These results suggest that functional inhibition by this autoantibody alone does not induce photoreceptor damage. Immunofluorescence in cultured cells might suggest that the antibody reacted with intracellular autoantigens released from damaged cells and concomitantly contributed to secondary inflammatory responses [39].

We cannot conclude how the autoantibody for fumarase, a ubiquitously expressed protein, specifically injures photoreceptor cells in DMO; similarly, the mechanism of antimitochondrial antibodies in primary biliary cirrhosis has not been determined [40]. Photoreceptor cells highly express fu-marase and are the main source of reactive oxygen species in diabetic states, which might promote an antigen-antibody reaction in these cells as discussed above [33, 34]. The absence of CD59 might allow complement-mediated autoimmune mechanisms in the photoreceptor inner and outer segments. In addition, the barrier properties of the retinal pigment epithelium and external limiting membrane might inhibit the diffusion of autoantibodies or complement components and cellular infiltration from or into the subretinal spaces and confine cellular damage to these layers [13].

Generally, intracellular autoantigens are released during non-apoptotic cell death, and the deposition of antigen-antibody complex subsequently exacerbates cellular damagevia several inflammatory mechanisms. Alternatively, anti-recoverin and anti-enolase antibodies from individuals with CAR are internalised into cells and induce cytotoxicity in the absence of complement [41, 42]. Histological findings in animal models led us to investigate complement-mediated mechanisms rather than inflammatory responses. Surprisingly, fumarase was recruited to the cell surface after complement treatment, and reacted to anti-

fumarase antibody derived from DMO sera with subsequent MAC formation, as in the case of autoantigens at the cell surface. Such changes depend on calcium signalling, although the downstream executioners remain to be elucidated. This result is consistent with the enigmatic finding that anti-fumarase antibody reacted with antigens in both photoreceptor inner and outer segments in mice administered with DMO sera, although immunostain- ing with the same sera was limited to the photoreceptor inner segments in untreated retinas. This is a novel molecular mechanism by which this autoantibody reacts to intracellular antigens on the cell surface. Future studies should elucidate whether sublytic MAC formation promotes the elicitation of autoimmune responses to intracellular autoantigens. Such biological changes are to some extent analogous to autoimmune responses to mitochondrial molecules in a few diseases [43].

Anti-fumarase antibody and complement impaired the structure and function of mitochondria. Generally, overload of calcium signalling damages mitochondria [23, 44], which allowed us to speculate that the persistent Ca^{2+} influx would contribute to mitochondrial injuries at least in part in cultured cells incubated with this autoantibody and complement. Mitochondrial disruption is one of the initial changes in neurodegenerative diseases [45]. In several pathological states, mitochondrial damage is one of the main regulators of synaptic plasticity [26]. Several mechanisms of mitochondrial damage are generally accepted: dysregulated Ca^{2+} levels, generation of reactive oxygen species, loss of mitochondrial membrane potential ($\Delta\psi m$) and efflux of apoptotic or necrotic factors, some of which have been shown in this study [26, 31, 45, 46]. The other mechanism is caspase activation. Several publications have reported that the pruning of axons and dendrites is mediated via a caspase cascade [25]. We thus speculated that caspase-3 activation partly contributed to the subcellular damage in the inner and outer segments, which corresponded to the dendrites specialised for photoreception.

Improvement in visual acuity is the primary endpoint for the efficacy ofanti-VEGF drugs for DMO, which is supported by the general surrogate marker of decreased macular thickness [12]. Recent publications have documented the restoration of the ellipsoid zone line on spectral domain OCT images after anti-VEGF therapy [47]. Re-establishment of the BRB by this standard treatment might decrease intraocular anti- fumarase IgG or complement components derived from the blood and concomitant photoreceptor damage. The decrease in this autoantibody might be consistent with photoreceptor restoration after treatment, although further studies should elucidate the underlying molecular mechanisms. A translational research study has demonstrated the involvement of complement under anti-VEGF treatment in age-related macular degeneration [48]. Future systematic and comparative studies may reveal the cellular and histological injuries induced by individual autoantibodies and/or complement in individual diseases [9, 10, 49, 50].

In conclusion, we have identified fumarase as a target of autoantibodies in a subgroup of DMO sera and a potential contributor to photoreceptor damage in DMO, although whether this autoantibody is the result of this pathogenesis remains to be elucidated. Further characterisation of autoantibodies against photoreceptor cells may facilitate the future development of antigen-specific immunomodulatory therapies for photoreceptor damage in DMO.

Supplementary Material

Refer to Web version on PubMed Central for supplementary material.

Acknowledgements

We would like to thank R. H. Rosa Jr (Texas A&M Health Science Center, Bryan, TX, USA) for providing discussion, and K. Okamoto-Furuta and H. Kohda (Division of Electron Microscopic Study, Center for Anatomical Studies, Graduate School of Medicine, Kyoto University, Kyoto, Japan) for technical assistance in electron microscopy.

Funding The study was supported by a Grant-in-Aid for Scientific Research from the Japan Society for the Promotion of Science (26462637, 17K11423, 18K19610). Immunostaining of human retinas, which used the Core Center for Vision Research funded by P30 EY007003 from the National Eye Institute, was supported by awards from Eversight and the Diabetes Consortium (National Institutes of Health). MS studies were performed at the Medical Research Support Center, Graduate School of Medicine, Kyoto University, which was supported by the Platform for Drug Discovery, Informatics, and Structural Life Science from the Ministry of Education, Culture, Sports, Science and Technology, Japan.

Abbreviations

BRB	Blood-retinal barrier
CAR	Cancer-associated retinopathy
COX	Cytochrome C oxidase
DMO	Diabetic macular oedema
HEK	Human embryonic kidney
logMAR	Logarithm of the minimum angle of resolution
MAC	Membrane attack complex
OCT	Optical coherence tomography
VEGF	Vascular endothelial growth factor

References

1. Frank RN (2004) Diabetic retinopathy. N Engl J Med 350(1):48–58. https://doi.oig/10.1056/NEJMra021678 [PubMed: 14702427]
2. Yau JW, Rogers SL, Kawasaki R et al. (2012) Global prevalence and major risk factors of diabetic retinopathy. Diabetes Care 35(3):556–564. 10.2337/dc11-1909 [PubMed: 22301125]
3. Gardner TW, Antonetti DA, Barber AJ, LaNoue KF, Levison SW (2002) Diabetic retinopathy: more than meets the eye. Surv Ophthalmol 47(Suppl 2):S253–S262. 10.1016/S0039-6257(02)00387-9 [PubMed: 12507627]
4. Antonetti DA, Klein R, Gardner TW (2012) Diabetic retinopathy. N Engl J Med 366(13):1227–1239. 10.1056/NEJMra1005073 [PubMed: 22455417]
5. Murakami T, Frey T, Lin C, Antonetti DA (2012) Protein kinase cß phosphorylates occludin regulating tight junction trafficking in vascular endothelial growth factor-induced permeability in vivo. Diabetes 61(6):1573—1583. 10.2337/db11-1367 [PubMed: 22438576]
6. Huang D, Swanson EA, Lin CP et al. (1991) Optical coherence tomography. Science 254(5035):1178—1181. https://doi.org/10.1126/science.1957169 [PubMed: 1957169]

7. Browning DJ, Glassman AR, Aiello LP et al. (2007) Relationship between optical coherence tomography-measured central retinal thickness and visual acuity in diabetic macular edema. Ophthalmology 114(3):525–536. https://doi.org/10.1016Zj.ophtha.2006.06.052 [PubMed: 17123615]
8. Spaide RF, Curcio CA (2011) Anatomical correlates to the bands seen in the outer retina by optical coherence tomography: literature review and model. Retina 31(8):1609–1619. 10.1097/IAE.0b013e3182247535 [PubMed: 21844839]
9. Sakamoto A, Nishijima K, Kita M et al. (2009) Association between foveal photoreceptor status and visual acuity after resolution of diabetic macular edema by pars plana vitrectomy. Graefes Arch Clin Exp Ophthalmol 247(10):1325–1330. 10.1007/s00417-009-1107-5 [PubMed: 19430805]
10. Murakami T, Nishijima K, Akagi T et al. (2012) Optical coherence tomographic reflectivity of photoreceptors beneath cystoid spaces in diabetic macular edema. Invest Ophthalmol Vis Sci 53(3):1506–1511. 10.1167/iovs.11-9231 [PubMed: 22323463]
11. Aiello LP, Avery RL, Arrigg PG et al. (1994) Vascular endothelial growth factor in ocular fluid of patients with diabetic retinopathy and other retinal disorders. N Engl J Med 331(22):1480–1487. https://doi.org/10T056/NEJM199412013312203 [PubMed: 7526212]
12. Cunningham ET, Jr, Adamis AP, Altaweel M et al. (2005) A phase II randomized double-masked trial of pegaptanib, an anti-vascular endothelial growth factor aptamer, for diabetic macular edema. Ophthalmology 112(10):1747–1757. 10.1016/j.ophtha.2005.06.007 [PubMed: 16154196]
13. Bunt-Milam AH, Saari JC, Klock IB, Garwin GG (1985) Zonulae adherentes pore size in the external limiting membrane of the rabbit retina. Invest Ophthalmol Vis Sci 26(10):1377–1380 [PubMed: 4044165]
14. Lo EH, Dalkara T, Moskowitz MA (2003) Mechanisms, challenges and opportunities in stroke. Nat Rev Neurosci 4(5):399–415. 10.1038/nrn1106 [PubMed: 12728267]
15. Thirkill CE, Roth AM, Keltner JL (1987) Cancer-associated retinopathy. Arch Ophthalmol 105(3): 372–375. 10.1001/archopht.1987.01060030092033 [PubMed: 2950846]
16. Ishida S, Yamashiro K, Usui T et al. (2003) Leukocytes mediate retinal vascular remodeling during development and vaso- obliteration in disease. Nat Med 9(6):781–788. 10.1038/nm877 [PubMed: 12730690]
17. Ambati J, Anand A, Fernandez S et al. (2003) An animal model of age-related macular degeneration in senescent Ccl-2- or Ccr-2- deficient mice. Nat Med 9(11):1390–1397. 10.1038/nm950 [PubMed: 14566334]
18. Srivastava R, Aslam M, Kalluri SR et al. (2012) Potassium channel KIR4.1 as an immune target in multiple sclerosis. N Engl J Med 367(2):115–123. 10.1056/NEJMoa1110740 [PubMed: 22784115]
19. Tolley E, Craig I (1975) Presence oftwo forms of fumarase (fumarate hydratase E.C. 4.2.1.2) in mammalian cells: immunological characterization and genetic analysis in somatic cell hybrids. Confirmation of the assignment of a gene necessary for the enzyme expression to human chromosome 1. Biochem Genet 13:867–883 [PubMed: 812482]
20. Early Treatment Diabetic Retinopathy Study Research Group (1985) Photocoagulation for diabetic macular edema. Early Treatment Diabetic Retinopathy Study report number 1. Arch Ophthalmol 103:1796–1806 [PubMed: 2866759]
21. Wilkinson CP, Ferris FL, 3rd, Klein RE et al. (2003) Proposed international clinical diabetic retinopathy and diabetic macular edema disease severity scales. Ophthalmology 110(9): 1677–1682. 10.1016/S0161-6420(03)00475-5 [PubMed: 13129861]
22. Triantafilou K, Hughes TR, Triantafilou M, Morgan BP (2013) The complement membrane attack complex triggers intracellular Ca2+ fluxes leading to NLRP3 inflammasome activation. J Cell Sci 126(13):2903–2913. 10.1242/jcs.124388 [PubMed: 23613465]
23. Rizzuto R, De Stefani D, Raffaello A, Mammucari C (2012) Mitochondria as sensors and regulators of calcium signalling. Nat Rev Mol Cell Biol 13(9):566–578. 10.1038/nrm3412 [PubMed: 22850819]
24. Elmore S (2007) Apoptosis: a review of programmed cell death. Toxicol Pathol 35(4):495–516. 10.1080/01926230701320337 [PubMed: 17562483]

25. Williams DW, Kondo S, Krzyzanowska A, Hiromi Y, Truman JW (2006) Local caspase activity directs engulfment of dendrites during pruning. Nat Neurosci 9(10): 1234—1236. 10.1038/nn1774 [PubMed: 16980964]
26. Mattson MP, Gleichmann M, Cheng A (2008) Mitochondria in neuroplasticity and neurological disorders. Neuron 60(5):748–766. 10.1016/j.neuron.2008.10.010 [PubMed: 19081372]
27. Funatsu H, Yamashita H, Noma H et al. (2002) Increased levels of vascular endothelial growth factor and interleukin-6 in the aqueous humor of diabetics with macular edema. Am J Ophthalmol 133(1): 70–77. 10.1016/S0002-9394(01)01269-7 [PubMed: 11755841]
28. Adamus G, Aptsiauri N, Guy J et al. (1996) The occurrence of serum autoantibodies against enolase in cancer-associated retinopathy. Clin Immunol Immunopathol 78(2):120–129. 10.1006/clin.1996.0021 [PubMed: 8625554]
29. Adamus G, Chew EY, Ferris FL, Klein ML (2014) Prevalence of anti-retinal autoantibodies in different stages ofage-related macular degeneration. BMC Ophthalmol 14(1):154 10.1186/1471-2415-14-154 [PubMed: 25488058]
30. Shechter R, London A, Schwartz M (2013) Orchestrated leukocyte recruitment to immune-privileged sites: absolute barriers versus educational gates. Nat Rev Immunol 13(3):206–218. 10.1038/nri3391 [PubMed: 23435332]
31. Nishikawa T, Edelstein D, Du XL et al. (2000) Normalizing mitochondrial superoxide production blocks three pathways of hyperglycaemic damage. Nature 404(6779):787–790. 10.1038/35008121 [PubMed: 10783895]
32. Sakaguchi S, Yamaguchi T, Nomura T, Ono M (2008) Regulatory T cells and immune tolerance. Cell 133(5):775–787. 10.1016/j.cell.2008.05.009 [PubMed: 18510923]
33. Du Y, Veenstra A, Palczewski K, Kern TS (2013) Photoreceptor cells are major contributors to diabetes-induced oxidative stress and local inflammation in the retina. Proc Natl Acad Sci U SA 110(41): 16586–16591. 10.1073/pnas.1314575110
34. Doyle HA, Mamula MJ (2001) Post-translational protein modifications in antigen recognition and autoimmunity. Trends Immunol 22(8):443–449. 10.1016/S1471-4906(01)01976-7 [PubMed: 11473834]
35. Saadoun S, Waters P, Bell BA et al. (2010) Intra-cerebral injection of neuromyelitis optica immunoglobulin G and human complement produces neuromyelitis optica lesions in mice. Brain 133(2):349–361. 10.1093/brain/awp309 [PubMed: 20047900]
36. Patrick J, Lindstrom J (1973) Autoimmune response to acetylcholine receptor. Science 180(4088): 871–872. 10.1126/science.180.4088.871 [PubMed: 4706680]
37. Toro JR, Nickerson ML, Wei MH et al. (2003) Mutations in the fumarate hydratase gene cause hereditary leiomyomatosis and renal cell cancer in families in North America. Am J Hum Genet 73(1): 95–106. 10.1086/376435 [PubMed: 12772087]
38. Pollard PJ, Spencer-Dene B, Shukla D et al. (2007) Targeted inactivation of fh1 causes proliferative renal cyst development and activation of the hypoxia pathway. Cancer Cell 11(4):311–319. 10.1016/j.ccr.2007.02.005 [PubMed: 17418408]
39. Hanayama R, Tanaka M, Miyasaka K et al. (2004) Autoimmune disease and impaired uptake of apoptotic cells in MFG-E8- deficient mice. Science 304(5674):1147–1150. 10.1126/science.1094359 [PubMed: 15155946]
40. Kaplan MM, Gershwin ME (2005) Primary biliary cirrhosis. N Engl J Med 353(12):1261–1273. 10.1056/NEJMra043898 [PubMed: 16177252]
41. Adamus G, Machnicki M, Seigel GM (1997) Apoptotic retinal cell death induced by antirecoverin autoantibodies ofcancer-associated retinopathy Invest Ophthalmol Vis Sci 38(2):283–291 [PubMed: 9040460]
42. Magrys A, Anekonda T, Ren G, Adamus G (2007) The role of anti- α-enolase autoantibodies in pathogenicity of autoimmune-mediated retinopathy J Clin Immunol 27(2):181–192. 10.1007/s10875-006-9065-8 [PubMed: 17235687]
43. Grundtman C, Kreutmayer SB, Almanzar G, Wick MC, Wick G (2011) Heat shock protein 60 and immune inflammatory responses in atherosclerosis. Arterioscler Thromb Vasc Biol 31(5):960–968. 10.1161/ATVBAHA.110.217877 [PubMed: 21508342]

44. Georgiannakis A, Burgoyne T, Lueck K et al. (2015) Retinal pigment epithelial cells mitigate the effects of complement attack by endocytosis of C5b-9. J Immunol 195(7):3382–3389. 10.4049/jimmunol.1500937 [PubMed: 26324770]

45. Swerdlow RH, Parks JK, Cassarino DS et al. (1998) Mitochondria in sporadic amyotrophic lateral sclerosis. Exp Neurol 153(1): 135–142. 10.1006/exnr.1998.6866 [PubMed: 9743575]

46. Galluzzi L, Blomgren K, Kroemer G (2009) Mitochondrial membrane permeabilization in neuronal injury. Nat Rev Neurosci 10(7): 481–494. 10.1038/nrn2665 [PubMed: 19543220]

47. Mori Y, Suzuma K, Uji A et al. (2016) Restoration of foveal photoreceptors after intravitreal ranibizumab injections for diabetic macular edema. Sci Rep 6(1):39161 10.1038/srep39161 [PubMed: 27966644]

48. Keir LS, Firth R, Aponik L et al. (2017) VEGF regulates local inhibitory complement proteins in the eye and kidney. J Clin Invest 127(1):199–214. 10.1172/JCI86418 [PubMed: 27918307]

49. Sawyer RA, Selhorst JB, Zimmerman LE, Hoyt WF (1976) Blindness caused by photoreceptor degeneration as a remote effect of cancer. Am J Ophthalmol 81(5):606–613. 10.1016/0002-9394(76)90125-2 [PubMed: 179323]

50. Ambati J, Atkinson JP, Gelfand BD (2013) Immunology of age-related macular degeneration. Nat Rev Immunol 13(6):438–451. 10.1038/nri3459 [PubMed: 23702979]

Research in context

What is already known about this subject?

- Diabetes disrupts the blood-retinal barrier, which sequesters retinal antigens from the autoimmune system
- Intraocular cytokines and infiltrated inflammatory cells promote neuroinflammation in diabetic retinopathy
- Neuroglial tissue, including photoreceptor cells, is impaired in diabetic macular oedema (DMO)

What is the key question?

- How is humoral autoimmunity elicited and how do autoantibodies against retinal antigens promote neuroglial impairment in DMO?

What are the new findings?

- Anti-fumarase antibody was identified in sera from individuals with DMO
- Anti-fumarase antibody is clinically related to vision reduction and photoreceptor damage in DMO
- Anti-fumarase antibody from participants with DMO, in concert with complement, was found to promote subcellular injuries to mouse photoreceptors and in cell culture

How might this impact on clinical practice in the foreseeable future?

- Anti-fumarase antibody could be a novel serum biomarker and serve as a potential target in the treatment of DMO

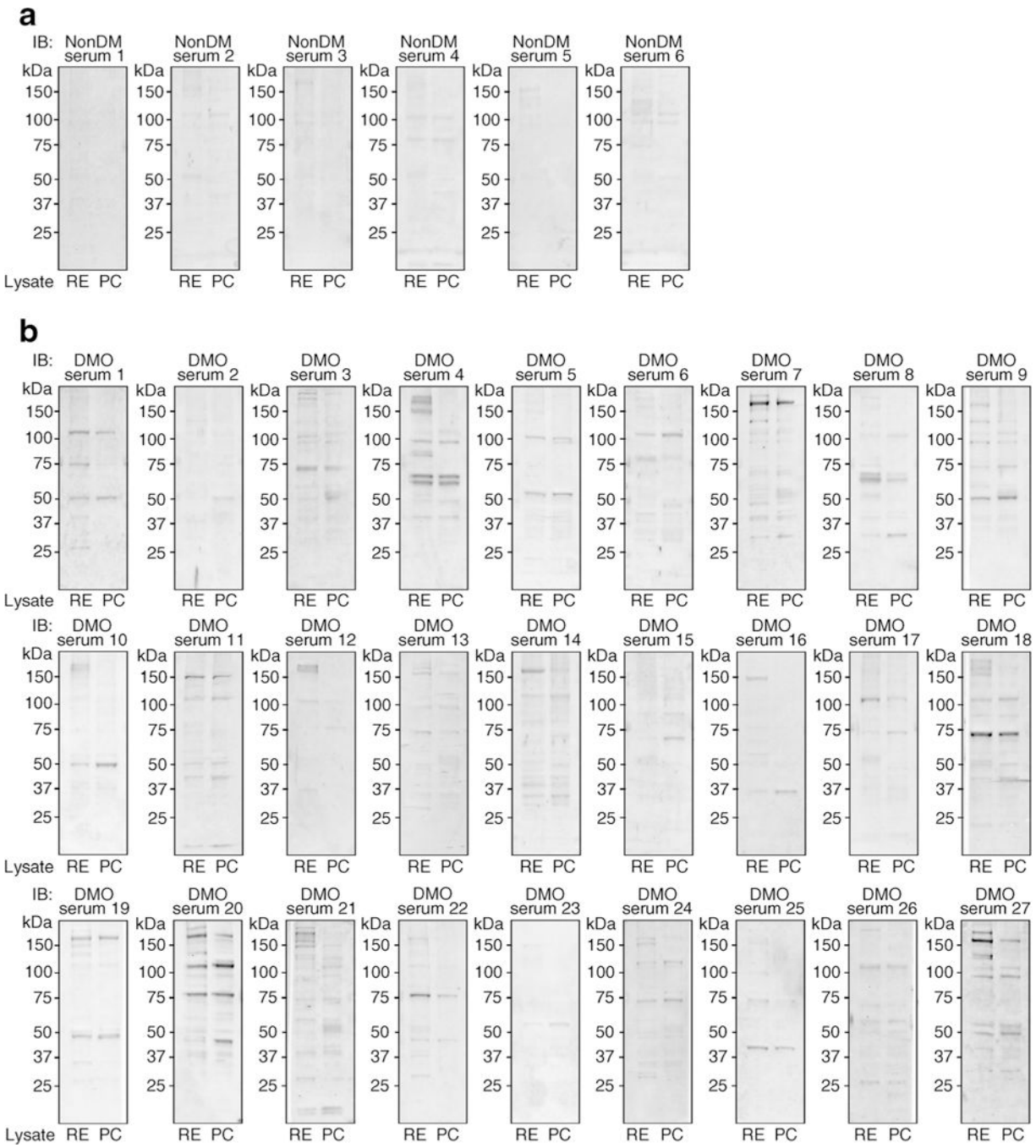

Fig. 1.

Reactivity of sera from non-diabetic (NonDM) or DMO participants with porcine retinal lysates (RE) and cell lysates of enriched photoreceptor cells (PC). Western blotting was used to screen the immuno-reactivity of serum IgG from six non-diabetic control participants (**a**) and 27 participants with DMO (b) to identify proteins expressed in photoreceptor cells. IB, immunoblot. Participants' characteristics are shown in ESM Table 1

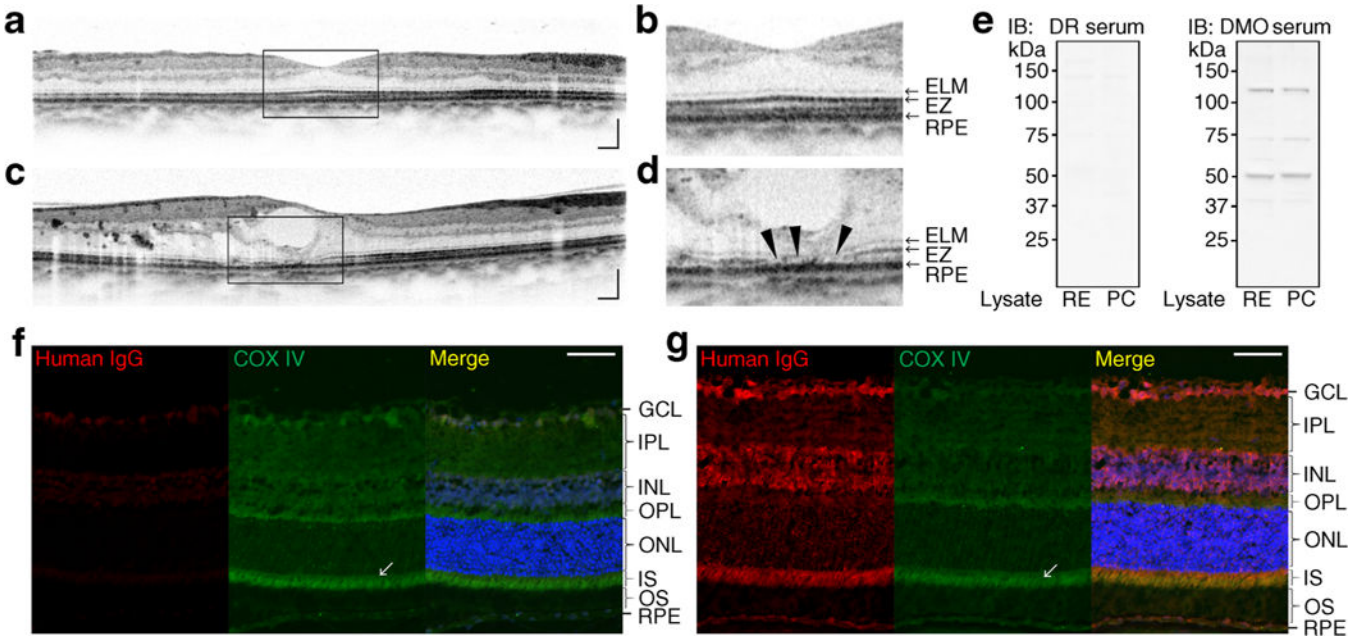

Fig. 2.

Autoantibodies in sera from participants with DMO. (**a-d**) OCT images revealed a definite ellipsoid zone line in an eye from a participant with diabetic retinopathy but not with DMO (**a**, **b**), compared with the lack of an ellipsoid zone (arrowheads) in parts of photoreceptor cells in an eye from a participant with DMO (**c**, **d**); scale bars, 200 μm. (b, d) Magnified images from (**a**) and (**c**), respectively. (e) Porcine retinal lysates (RE) and cell lysates of enriched photoreceptor cells (PC) underwent immunoblotting (IB) with serum IgG from the same participants as in (**a-d**). (**f**, **g**) Immunofluorescence showed no immunoreactivity of serum IgG from the participant with diabetic retinopathy but without DMO in photoreceptor cells of C57BL/6 mice (n = 2 retinas) (**f**), compared with co-localisation of COX IV with serum IgG from the same DMO participant at the ellipsoid zone of photoreceptor inner segments (arrows in **f** and **g**; n = 2 retinas) (**g**); scale bars, 50 μm. DR, diabetic retinopathy; ELM, external limiting membrane; EZ, ellipsoid zone; GCL, ganglion cell layer; INL, inner nuclear layer; IPL, inner plexiform layer; IS, inner segment; ONL, outer nuclear layer; OPL, outer plexiform layer; OS, outer segment; RPE, retinal pigment epithelium. Participants' characteristics are shown in ESM Table 2

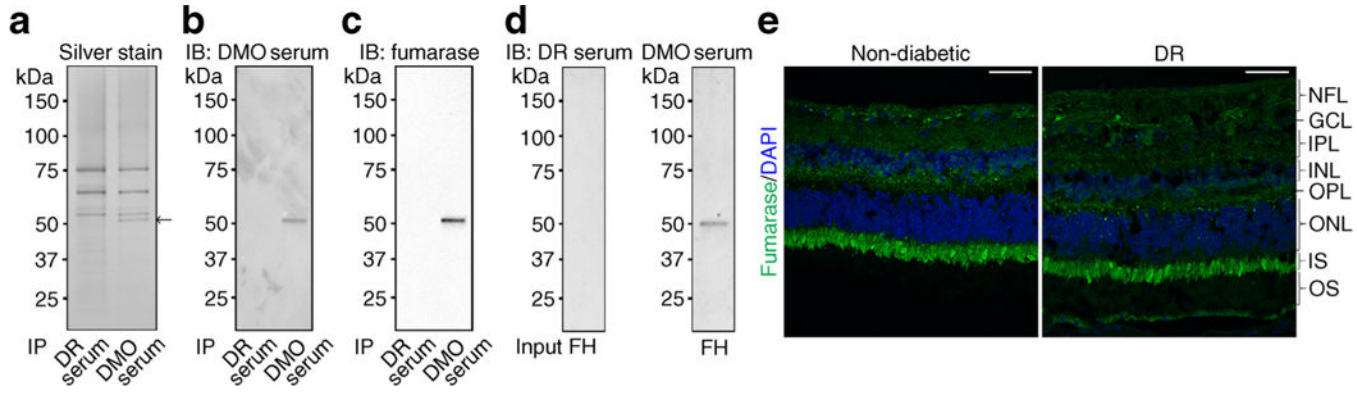

Fig.3.

Identification of fumarase as a target of serum IgG from participants with DMO. (**a**, **b**) SDS-PAGE analysis of porcine photoreceptor cell lysates precipitated with serum IgG of a participant with diabetic retinopathy without (DR serum) or with (DMO serum) DMO, whose characteristics are shown in ESM Table 3, was followed by either silver staining (**a**) or immunoblotting (IB) with serum IgG from the same DMO participant (**b**). (**c**) Analysis of the approximately 50 kDa unique band (arrow in a) using MS-identified fumarase, which was confirmed by reblotting with mouse monoclonal anti-fumarase antibodies. (**d**) Human recombinant fumarase (FH) was analysed by immunoblotting with IgG from DR or DMO serum. (**e**) Immunostaining revealed the immunoreactivity of fumarase in the photoreceptor inner segments in retinas from individuals without diabetes and from those with diabetic retinopathy (the donors' characteristics are shown in ESM Table 4; representative images of six non-diabetic donors and five with diabetic retinopathy are shown); scale bars, 50 μm. GCL, ganglion cell layer; INL, inner nuclear layer; IP, immunoprecipitation; IPL, inner plexiform layer; IS, inner segment; NFL, nerve fibre layer; ONL, outer nuclear layer; OPL, outer plexiform layer; OS, outer segment

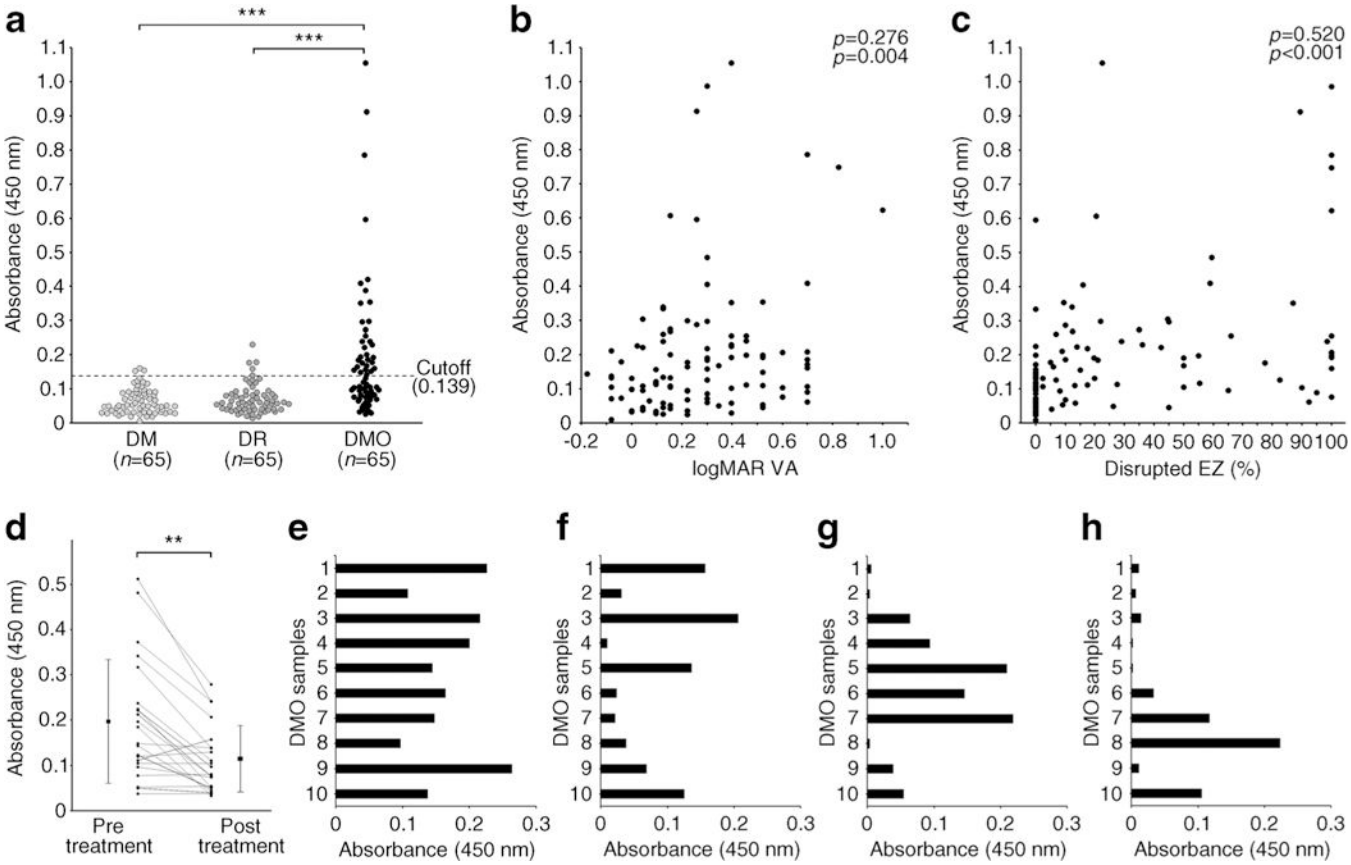

Fig. 4.

Quantitative analysis of IgG reactivity to recombinant fumarase in serum or vitreous humour from participants with DMO. (**a**) ELISA was used to quantify the titres of total anti-fumarase autoantibodies, which revealed higher titres in DMO sera than in sera from participants with diabetes mellitus without diabetic retinopathy (DM) or those with diabetic retinopathy without DMO (DR). ****p* <0.001, Kruskal-Wallis test of one-way ANOVA with Dunnett's multiple comparison; *n* = 65 in individual groups. Participants' characteristics are shown in ESM Table 5. (b, c) Post hoc analyses of 106 DMO eyes from two datasets after excluding those with media opacity affecting visual acuity The titre was modestly associated with logMAR visual acuity (VA) (**b**) and with the transverse length of disrupted ellipsoid zone (EZ) (**c**). Spearman's rank correlation coefficient. Participants' characteristics are shown in ESM Table 7. (**d**) Reduced titres of anti-fumarase IgG after anti-VEGF treatment for DMO. ***p* = 0.001, Wilcoxon signed-rank test; *n* = 21. Participants' characteristics are shown in ESM Table 8. (**e**-**h**) Titres of individual IgG subtypes of fumarase-specific antibodies in ten sera with higher titres of total IgG in (**a**). (**e**) IgG1, (f) IgG2, (**g**) IgG3 and (**h**) IgG4. Most sera contained higher titres of IgG1 and/or IgG3 against fumarase. Participants' characteristics are shown in ESM Table 9

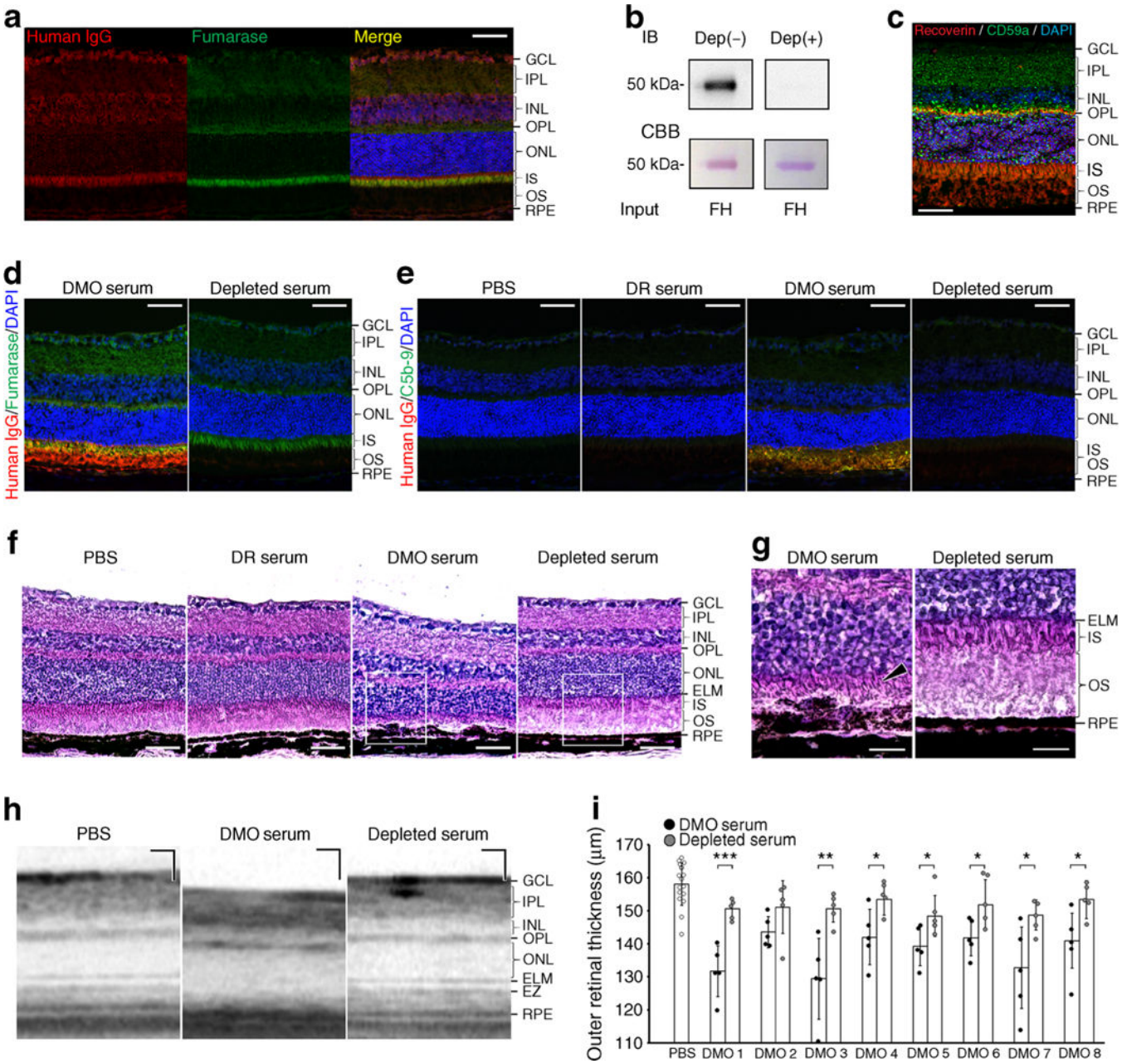

Fig. 5.

Anti-fumarase antibody in DMO serum is necessary for complement activation and structural changes in photoreceptor inner and outer segments in C57BL/6 mice administered with DMO sera. (**a**) Untreated retinas immunostained with DMO serum containing higher titres of anti-fumarase IgG (ESM Table 10), which were to be subretinally injected; representative images of $n = 3$ retinas; scale bar, 50 μm. (**b**) Western blot using the same DMO serum as in (**a**), with and without depletion (dep[+] and dep[–], respectively); $n = 3$ of duplicate ELISAs. (**c**) No or weak immunoreactivity of CD59a, an endogenous inhibitor of MAC, in photoreceptor inner and outer segments of untreated retinas; representative images of $n = 3$ retinas; scale bar, 50 μm. (**d-i**) Retinal status was analysed 24 h (**d**, **e**) or 7 days (f-i)

after subretinal administration of DMO serum containing higher titres of anti-fumarase IgG or serum depleted of anti-fumarase antibody. (**d**, **e**) Immunofluorescence analysis of IgG from DMO serum in mouse photoreceptor inner and outer segments, compared with fumarase and C5b-9. Representatives of sera from two participants with diabetic retinopathy and two with DMO (ESM Table 10) are shown. Haematoxylin and eosin staining (**f**, **g**) and OCT images (**h**) revealed structural damage in the photoreceptor inner and outer segments in mouse eyes injected with DMO serum, and this damage was partially reversed by depleted serum; scale bars, 50 μm (f, h) and 20 μm (g). Representatives of sera from four participants with diabetic retinopathy and eight with DMO (ESM Table 10) are shown. (i) OCT measurement of the outer retinal thickness (from the outer plexiform layer to the Bruch's membrane) in retinas injected with DMO sera (ESM Table 10; DMO 1–8). $*p<0.05$, $**p<0.01$, $***p<0.001$; $n = 16$ in PBS, $n = 5$ in each group; paired t test. CBB, Coomassie Brilliant Blue; ELM, external limiting membrane; FH, human recombinant fumarase; GCL, ganglion cell layer; INL, inner nuclear layer; IPL, inner plexiform layer; IS, inner segment; ONL, outer nuclear layer; OPL, outer plexiform layer; OS, outer segment; RPE, retinal pigment epithelium

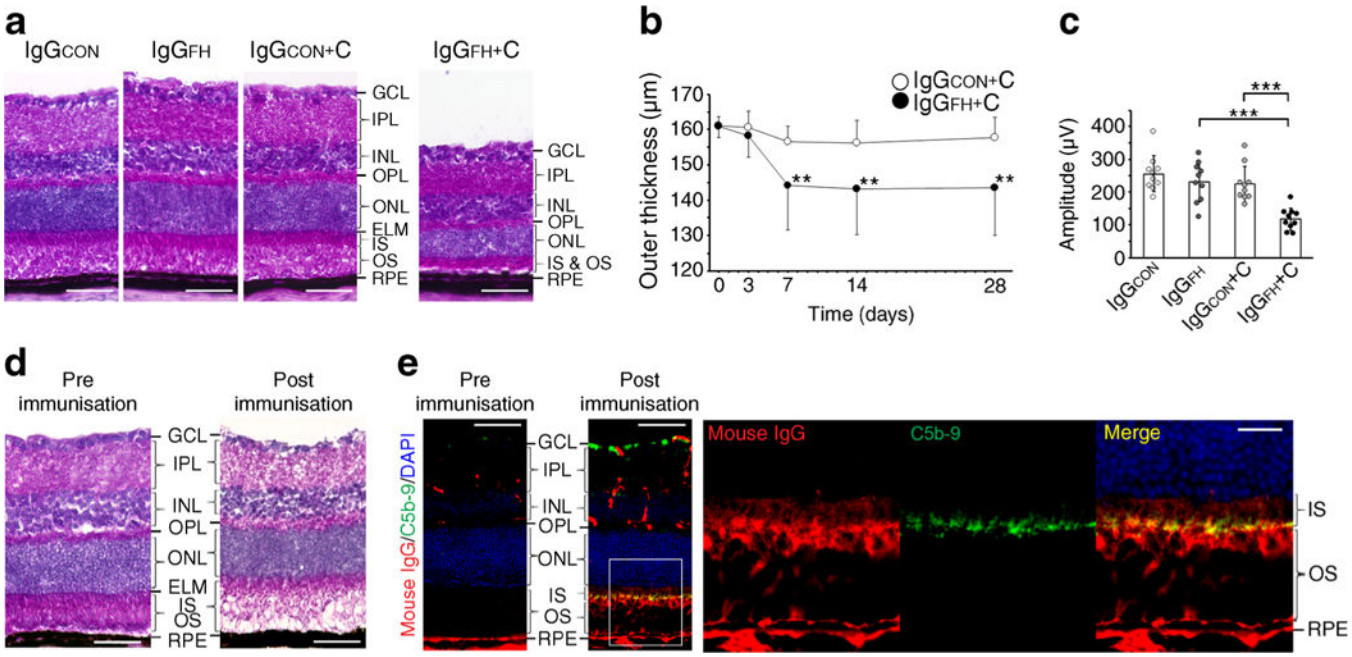

Fig. 6.

Anti-fumarase antibody in DMO sera in combination with complement promotes cellular injuries in animal models. (**a**-**c**) Morphologic and functional analyses of retinas 7 days after the administration of 4 mg/ml IgG + 50% complement into the subretinal spaces of C57BL/6 mice (passive transfer model). Haematoxylin and eosin staining (**a**). C, complement from three individuals without diabetes (ESM Table 10); $IgG_{CON,}$ control IgG from sera from four participants with diabetic retinopathy without DMO (ESM Table 10; 0.049 arbitrary units [AU] in 4 mg/ml); IgG_{FH}, affinity-purified anti-fumarase IgG from sera from four participants with DMO (ESM Table 10; 0.417 AU in 4 mg/ml); n =10 retinas; scale bars, 50 μm. (b) OCT measurements revealed significant decreases in the outer retinal thickness at 7, 14 and 28 days after administration of IgGpH + C (p <0.01 vs baseline); n = 15 retinas; ** p <0.01 for the comparison between the two groups at each time point, one-way ANOVA with Bonferroni correction. (**c**) Amplitude of the a-wave of electroretinograms in each group; *** p <0.001, one-way ANOVA with Bonferroni correction; n =10 retinas. (**d**, **e**) Active immunisation with fumarase of B10.RIII mice (active immunisation model). (**d**) Haematoxylin and eosin staining showed that the photoreceptor inner and outer segments were damaged in six of 14 (42.9%) mice. Scale bar, 50 μm. (**e**) Immunostaining revealed immunoreactivity to mouse IgG in the inner and outer segments of photoreceptor cells, with which C5b-9 was partly co-localised; scale bar, 50 or 20 μm (magnified images). ELM, external limiting membrane; GCL, ganglion cell layer; INL, inner nuclear layer, IPL, inner plexiform layer; IS, inner segment; ONL, outer nuclear layer; OPL, outer plexiform layer; OS, outer segment; RPE, retinal pigment epithelium

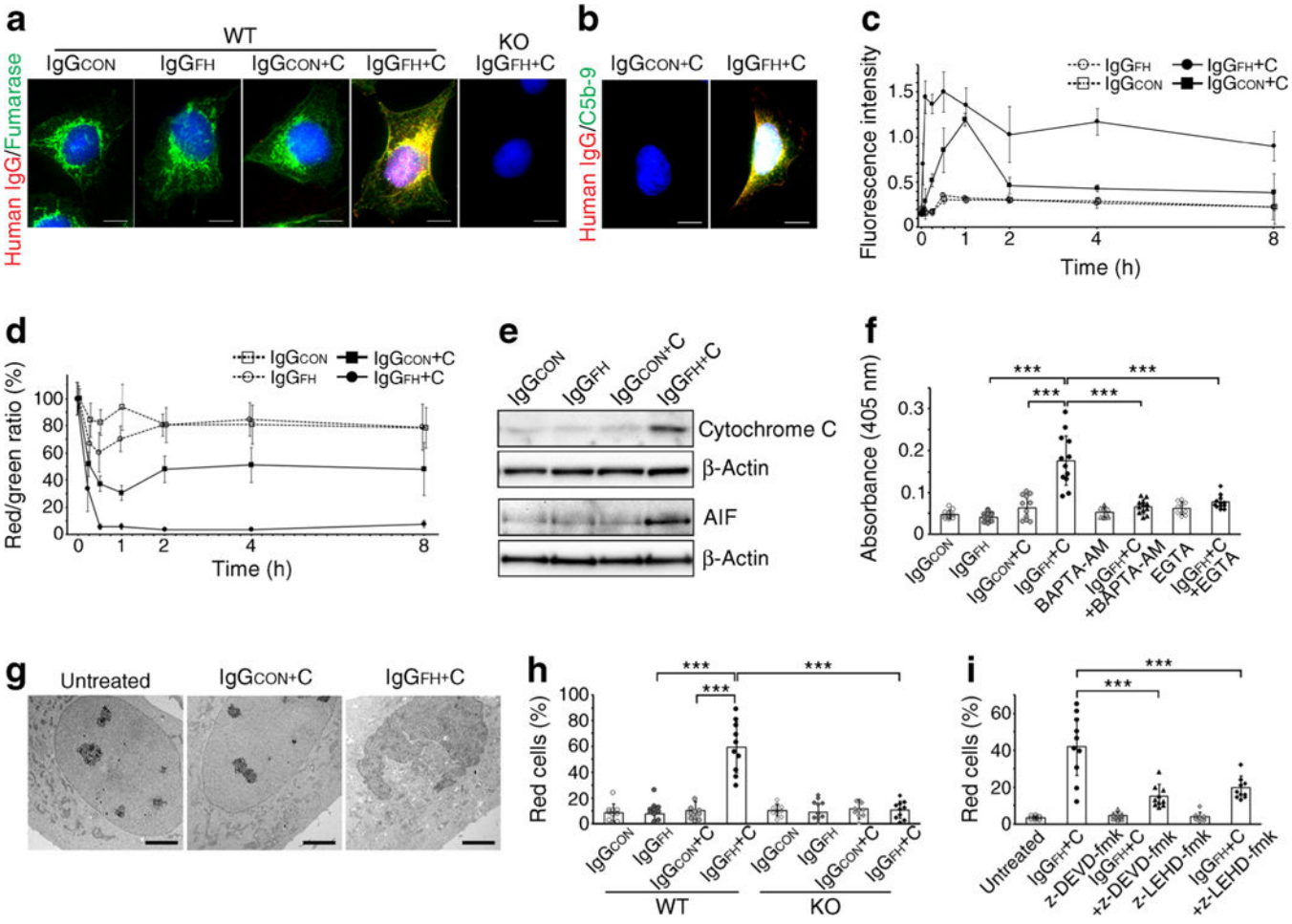

Fig. 7.

Anti-fumarase antibody from DMO sera in concert with complement reacts to autoantigens on the cell surface and promotes cellular injuries in cultured cells. (**a**, **b**) Immunofluorescence of HEK 293 cells incubated with affinity-purified anti-fumarase IgG from DMO sera (1 mg/ml) and complement (5%) for 3 h; $n = 3$; scale bars, 10 μm. Wild-type (WT) = $FH^{+/+}$ HEK 293 cells. Knockout (KO) = $FH^{-/-}$ HEK 293 cells. (**c**) Increased intracellular Ca^{2+} concentration in 661W cells treated with IgG_{FH} + C ($p < 0.001$ vs IgG_{FH} or IgG_{CON} + C); $n = 6$. (**d**) The JC-1 red/green ratio decreased at 30 min or later in HEK 293 cells treated with IgG_{FH} + C ($p < 0.001$ vs IgG_{FH} or IgG_{CON} + C); $n = 6$. (**e**) Immunoblot of the cytosolic fraction isolated from 661W cells; $n = 8$. (f) Colorimetry assay revealed that IgG_{FH} + C increased caspase-3 activity in 661W cells. ***$p<0.001$. $n = 10–12$. (g) Electron microscope image of HEK 293 cells 24 h after incubation; $n = 3$. Scale bars, 5 μm. (h) Dead cells (ethidium homodimer-1-positive red cells) after 24 h incubation in HEK 293 cells; ***$p < 0.001$; $n = 10$. (**i**) Cell death partly depended on caspase-3 activation in 661W cells; ***$p < 0.001$; $n = 10$. One-way ANOVAwith Bonferroni correction in (**c**), (**d**), (**f**), (**h**) and (**i**). AIF, apo-ptosis-inducing factor; BAPTA-AM, *O,O'*-Bis(2-aminophenyl) ethyleneglycol-*N,N,N',N'*-tetraacetic acid, tetraacetoxymethyl ester; C, complement; IgG_{CON}, control IgG; IgG_{FH}, affinity-purified anti-fumarase IgG; z-DEVD-fmk, *N*-[(phenylmethoxy)carbonyl]-L-α-aspartyl-L-μ- glutamyl-*N*-[(1S)-3-fluoro-1-(2-methoxy-2-oxoethyl)-2-oxopropyl]-L-

alinamide, 1,2-dimethyl ester; z-LEHD-fmk, methyl (4*S*)-5-[[(2*S*)-1-[[(3*S*)-5-fluoro-1-methoxy-1,4-dioxopentan-3-yl]amino]-3-(1H- imidazol-5-yl)-1-oxopropan-2-yl]amino]-4-[[(2*S*)-4-methyl-2- (phenylmethoxycarbonylamino)pentanoyl]amino]-5-oxopentanoate